ISBN: 978-3-95450-219-6 ISSN: 2226-0366 doi: 10.18429/JACoW-LINAC2024-THPB041

CALIBRATION OF THE ANALOG BEAM-SIGNAL HARDWARE FOR THE CREDITED ENGINEERED BEAM POWER LIMIT SYSTEM AT THE PROTON POWER UPGRADE PROJECT AT THE SPALLATION NEUTRON SOURCE*

C. E. Deibele†, M. Bobrek, P. Bong, K. Kasemir, K. Mahoney, C. Michaelides, Y. Tan, D. Willis
Oak Ridge National Laboratory, Oak Ridge, TN, USA
T. Allison, Osprey Digital Control Systems, Ocean City, MD, USA
C. Barbier, ITER, St. Paul-lez Durance, France

Abstract

A programmable signal processor-based credited safety control that calculates pulsed beam power based on beam kinetic energy and charge was designed as part of the Proton Power Upgrade (PPU) project at the Spallation Neutron Source (SNS). The system must reliably shut off the beam if the average power exceeds 2.145 MW averaging over 60 seconds. System calibration requires pedigree in measurements, calibration setup, and calculations. This paper discusses the calibration of the analog beam signal components up to and including the Analog Digital Convertors (ADCs) for implementation into the Safety Programmable Logic Controllers (PLCs) and Field Programmable Gate Arrays (FPGAs).

BLOCK DIAGRAM

The Beam Power Limit System (BPLS) block diagram in Fig. 1 shows redundancy in the beam current measurement with two chains, each beginning with a Fast Current Transformer (FCT) [1]. The FCTs are connected to long-haul cables that send the beam signal to an Analog Front End (AFE). Each AFE conditions the beam signal and distributes it to two different Analog to Digital Convertors (ADCs). One ADC is contained within the Digital Processing Unit (DPU), which is part of the credited Personnel Protection System (PPS), and the other is sent to the Protection System Interface (PSI) which is a Machine Protection System (MPS).

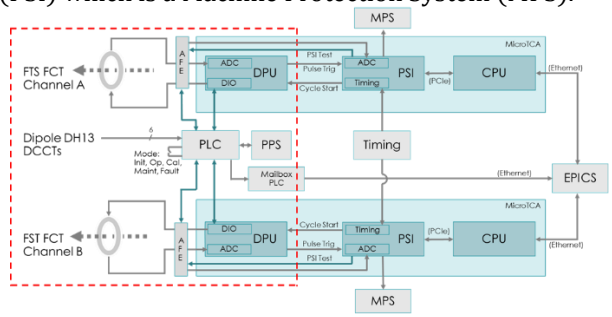

Figure 1: Block Diagram of BPLS.

The Safety Programmable Logic Controller (PLC) measures the beam energy through a calculation from six individual Direct Current-Current Transformers (DCCTs) [2] measurements. The DCCTs measure the dipole current used to steer the beam to the target station. The DCCTs are calibrated with the vendor.

One salient difference between the credited PPS system measurement and the non-credited MPS measurement is the use of timing. Timing is used in the MPS measurement to supply a gate to measure the beam signal, while the PPS system runs independently of timing.

The following equation [3] is used to calculate the beam charge trip limit (counts):

$$Limit = (1 + s_{11})T_{AFE}T_{cable}Z_{FCT}\frac{NP_{limit}}{k_{ADC}E\,\Delta t},$$

where s_{11} is the reflection looking into the ADC, T_{AFE} and T_{cable} are the transmission coefficients of the AFE and long haul cable respectively, Z_{FCT} is the transimpedance of the FCT, N is the number of seconds to average over, P_{limit} is the threshold power, k_{ADC} is the volts/count conversion of the ADC, E is the energy of the beam, and Δt is the sample rate of the ADC. This results in Limit being in units of counts, which is provided to the DPU and PSI where the beam charge algorithms and trip comparisons are implemented in Field Programmable Gate Arrays (FPGAs).

For the purpose of this paper, the FCT transimpedance, long-haul cable transmission, AFE transmission, and ADC conversion factor require calibration so that appropriate trip limits can be assigned as necessary. The quantities of the number of seconds N, the power limit P_{limit}, and sample rate Δt are fixed.

FCT CALIBRATION

The FCT transimpedance is nominally designed to be 0.25 Ω at the factory. Parasitic elements in its manufacture add to deviations in the design value and therefore requires to be calibrated.

To perform this calibration [4, 5], a set of cone-shaped launches were designed to transition from a cable to the geometry consistent with the FCT. Figure 2 shows two launches that are assembled onto a long section of coax that is short circuited. The long coax is used to characterize each launch independently, so that they can be re-assembled with the FCT placed in-between.

* This material is based upon work supported by the U.S. Department of Energy, Office of Science and by UT-Battelle, LLC, under contract DE-AC05-00OR22725
† deibele@ornl.gov

ISBN: 978-3-95450-219-6 ISSN: 2226-0366 doi: 10.18429/JACoW-LINAC2024-THPB041

Characterization of a single launch is performed by measuring the reflection of the launch plus long coax section. With the end of the structure shorted, the effects of the launch occur temporally before the short at the end of the coax. An example of the measurement is shown in Fig. 3.

The ungated measurement is the red trace is the raw reflection signal converted to the time domain. The large negative pulse is the reflection at the end of the coax represents the short-circuit. The small oscillations, near t=0 are effects due to the launch. The blue trace is gated and this mathematically removes the short circuit so that the launch can be modeled.

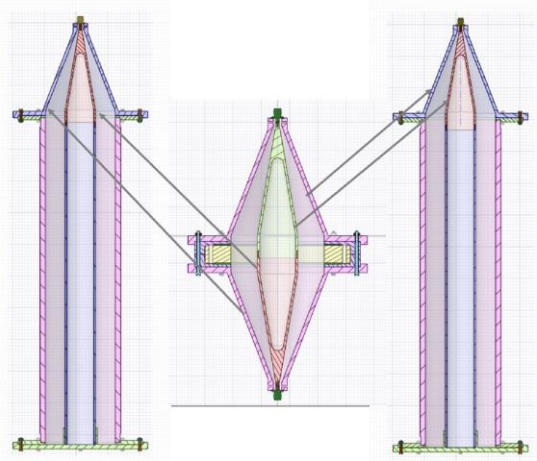

Figure 2: Launch sections used in calibration of FCT.

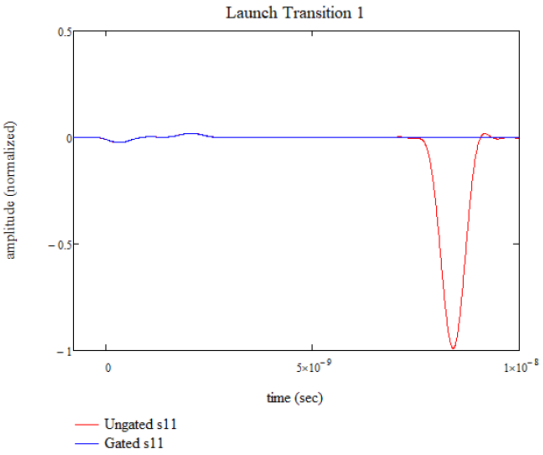

Figure 3: Measurement of reflection of launch.

The gated measurements are then converted back to the frequency domain and saved as a Touchstone-format .s1p file [6]. The gated data was then optimized using an RF design tool, as part of the Ansys Electronics Desktop [7]. Figure 4 shows a resulting optimization.

The FCT was then assembled with the two launches, shown schematically as the center component of Fig. 2. A full 4-port measurement was then performed. The FCT has two ports of its own, the main winding and calibration winding, and each launch has a port.

Optimization of the 4-port measurement is shown in Fig. 5. The top part of Fig. 5 shows the 4-port measurement, while the bottom of Fig. 5 shows the optimization. Components for measuring the current and voltage at the center transmission line is included.

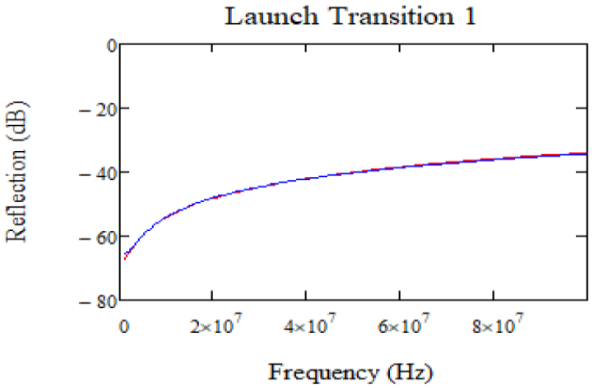

Figure 4: Modeled (blue) vs Measured (red) launch.

The transimpedance was then calculated by the calculated current in Fig. 5 and the measured transmission through the main winding of the FCT from the launch. A plot of the transimpedance of the FCT is shown in Fig. 6.

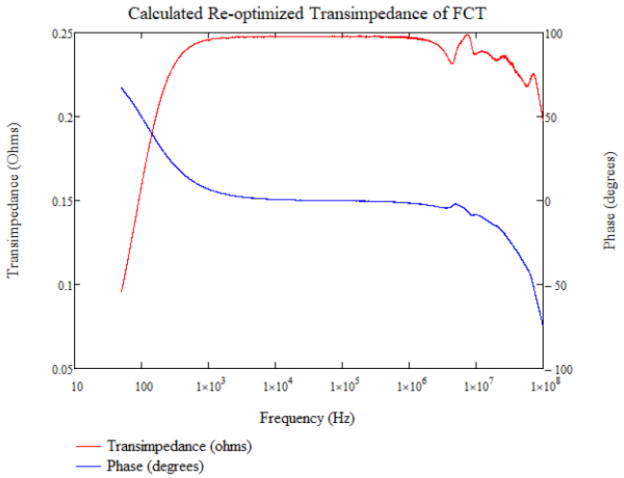

Figure 6: Transimpedance of the FCT.

LONG HAUL CABLE CALIBRATION

The transmission of the cable, s_{21}, can be calculated from the use of a series of reflection measurements, s_{11} [8], where the cable is open and short circuited. The reflection of the open, s_{11}^o, and short-circuited, s_{11}^s, cables can be approximated as a function of transmission in the following two equations:

$$s_{11}^o(\omega) = s_{21}^o(\omega)s_{21}^o(\omega)$$
$$-s_{11}^s(\omega) = s_{21}^s(\omega)s_{21}^s(\omega)$$

These equations are valid only when the reflection of the long-haul cable is small with respect to the transmission of the cable. The right-hand side of these equations show that the signal propagates to and from the open and short circuit. Unwrapping the measurement results in the following

$$\rightarrow s_{21}^o(\omega) = |s_{11}^o(\omega)|^{0.5} e^{0.5\, i\, arg\{s_{11}^o\{\omega\}\}}$$
$$\rightarrow s_{21}^s(\omega) = |s_{11}^s(\omega)|^{0.5} e^{0.5\, i\, arg\{-s_{11}^s\{\omega\}\}}$$

ISBN: 978-3-95450-219-6 ISSN: 2226-0366 doi: 10.18429/JACoW-LINAC2024-THPB041

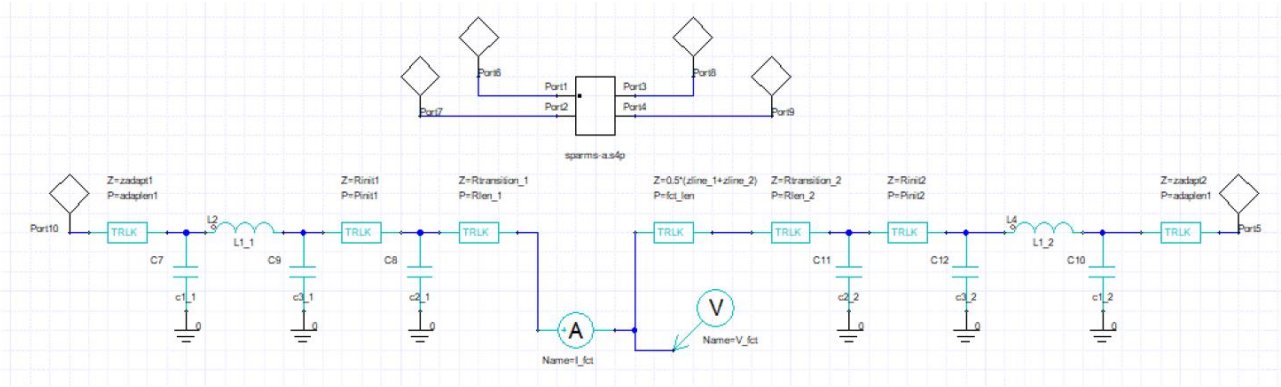

Figure 5: Optimization setup for the 4-port measurement of the FCT with launches.

The delay of the cable is then calculated and the open and short circuit transmission results in Fig. 7.

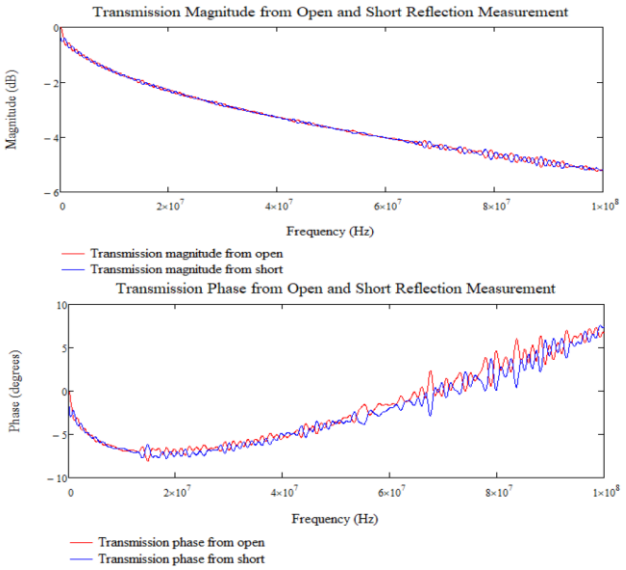

Figure 7: Transmission open vs short comparison.

The calculation of transmission with the two methods results in small oscillations which are out of phase from one another. This is caused by resonances of the interconnects and the physical length of the cable. The average of these two measurements (real and imaginary) result in the calibrated transmission of the long haul cables as shown in Fig. 8

DISPERSION CORRECTION

The dispersive properties of the FCT shown in Fig. 5 and the cable shown in Fig. 8 were corrected using Finite Impulse Response (FIR) filters [9, 10]. The number of taps for each equalizer was determined by using a set of test functions and convolving the test functions with the impulse response of the cable or transimpedance and then likewise convolving the equalizer.

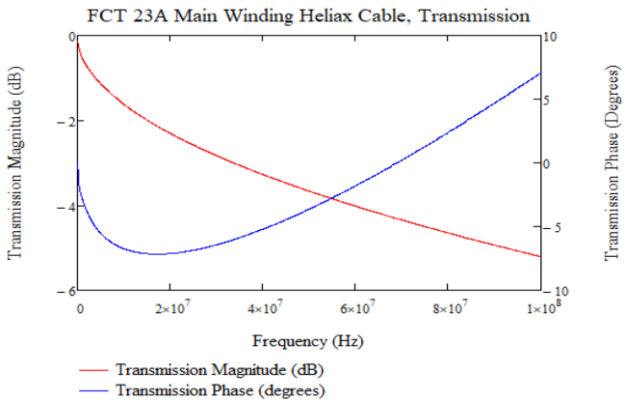

Figure 8: Calibrated cable magnitude and phase.

The taps for each equalizer were hard coded into the DPU and PSI FPGA code. Fixed coefficients were used in the PLC to control the average value of the calibration. A plot of the equalizer values is shown in Fig. 9.

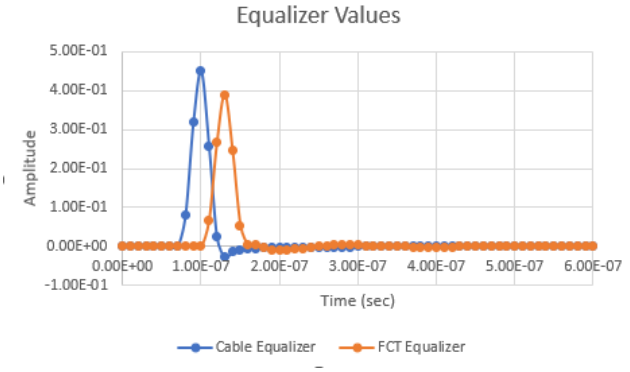

Figure 9: Plot of equalizer values.

REFERENCES

[1] Bergoz Instrumentation, CT-CF12"-198.4-40-UHV-CAW1-N-THH.

[2] "GMW Associates," DCCT CPCO-4000-160-MA.

[3] "Beam Power Limit System (BPLS) Calculation of Average Power," P04060200-CAC-100002-R00, unpublished.

[4] "Calibration of the Launches for the Beam Power Limit System Fast Current Transformer Calibration Stand," P04060200-CAL10003-R00, unpublished.

ISBN: 978-3-95450-219-6 ISSN: 2226-0366 doi: 10.18429/JACoW-LINAC2024-THPB041

[5] "Calibration of Bergoz Serial #3906 Fast Current Transformer Beam Power Limit System," P04060200-CAL10002-R00, unpublished.

[6] Touchstone file, https://en.wikipedia.org/wiki/Touchstone_file

[7] Ansys, http://www.ansys.com

[8] "Heliax Cable Calibration for the Beam Power Limit System," P04060200-CAL10000-R00, unpublished.

[9] "Heliax Cable Finite Impulse Response Coefficient Calculation for the Beam Power Limit System," P04060200-CAC10001-R00, unpublished.

[10] "Fast Current Transformer Finite Impulse Response Coefficient Calculation for the Beam Power Limit System," P04060200-CAC10003-R00, unpublished.